

IL-1 α cleavage by inflammatory caspases of the non-canonical inflammasome controls the senescence-associated secretory phenotype.

Kimberley A. Wiggins¹, Aled J. Parry², Liam D. Cassidy², Melanie Humphry¹, Steve J. Webster^{3#}, Jane C. Goodall³, Masashi Narita² Murray CH. Clarke^{1*}

¹Division of Cardiovascular Medicine,
³Division of Rheumatology,
Department of Medicine, and
²Cancer Research UK Cambridge Institute,
University of Cambridge,
Addenbrooke's Hospital,
Cambridge,
CB2 0QQ,
UK.

***For correspondence:**
Email: mchc2@cam.ac.uk
Telephone: (44) 1223 762581
Fax: (44) 1223 331505

[#]Current address: Department of Veterinary Medicine, Madingley Road, Cambridge, CB3 0ES.

Short running title: Caspase-5/11 cleavage of IL-1 α controls the SASP.

ABSTRACT

Interleukin-1 alpha (IL-1 α) is a powerful cytokine that modulates immunity, and requires canonical cleavage by calpain for full activity. Mature IL-1 α is produced after inflammasome activation and during cell senescence, but the protease cleaving IL-1 α in these contexts is unknown. We show IL-1 α is activated by caspase-5 or -11 cleavage at a conserved site. Caspase-5 drives cleaved IL-1 α release after human macrophage inflammasome activation, while IL-1 α secretion from murine macrophages only requires caspase-11, with IL-1 β release needing caspase-11 and -1. Importantly, senescent human cells require caspase-5 for the IL-1 α -dependent senescence-associated secretory phenotype (SASP) *in vitro*, while senescent mouse hepatocytes need caspase-11 for the SASP-driven immune surveillance of senescent cells *in vivo*. Together, we identify IL-1 α as a novel substrate of non-canonical inflammatory caspases, and finally provide a mechanism for how IL-1 α is activated during senescence. Thus, targeting caspase-5 may reduce inflammation and limit the deleterious effects of accumulated senescent cells during disease and aging.

INTRODUCTION

Inflammation has evolved to protect the host from acute insults such as infection or physical injury. However, chronic inflammation is associated with many age-related diseases such as atherosclerosis, osteoarthritis, and cancer. Senescent cells that drive inflammation also play pivotal roles in these diseases (Childs et al., 2016; Jeon et al., 2017; T. W. Kang et al., 2011), and naturally accumulate in tissues during aging (Baker et al., 2016). Strikingly, removal of senescent cells can prevent development of disease and also reverse natural features of aging (Baker et al., 2016; Baker et al., 2011; Childs et al., 2016; Jeon et al., 2017; T. W. Kang et al., 2011). Thus, understanding how senescence drives inflammation is of critical importance in health, disease and aging.

Senescence is a protective mechanism that induces permanent cell cycle arrest to prevent transmission of defects to the next generation, particularly to stop malignant transformation. Replicative senescence occurs after repeated cell division critically shortens telomeres, while induced senescence occurs after oncogene activation, mitochondrial deterioration, oxidative stress or DNA damage (Munoz-Espin & Serrano, 2014). As aging drives tumorigenesis and telomere shortening, it induces senescence via both pathways. Most senescent cells develop altered secretory activities known as a senescence-associated secretory phenotype (SASP). The SASP releases proinflammatory cytokines (e.g. IL-1, IL-6) and chemokines (e.g. IL-8, GRO α), growth factors (e.g. G-CSF, bFGF), and proteases (e.g. MMPs, PAI-1) (Coppe et al., 2008), conferring diverse activities. Thus, although cell cycle arrest during senescence limits cancer and the SASP instructs clearance of pre-neoplastic cells (T. W. Kang et al., 2011), this is balanced against establishment of a chronic inflammatory microenvironment that can damage tissue, drive disease and promote tumorigenesis if senescent cells persist (Grivnickov, Greten, & Karin, 2010). IL-1 α acts in an autocrine/paracrine fashion to drive the SASP (Gardner, Humphry, Bennett, & Clarke, 2015; Orjalo, Bhaumik, Gengler, Scott, & Campisi, 2009), with upstream expression controlled in part by ATM/ATR liberation of GATA4 from p62-directed autophagy (C. Kang et al., 2015) and/or an mTORC1-dependent pathway (Lagerge et al., 2015). However, how IL-1 α is cleaved, activated or released during senescence to enable it to drive the SASP is unknown.

Interleukin-1 (IL-1) is an ancient cytokine that exerts effect on both innate and adaptive immunity. IL-1 α and β are the principal ligands that bind to the type 1 IL-1 receptor (IL-1R1), causing recruitment of the IL-1 receptor accessory protein (IL-1RAP) and subsequent interaction with the signalling adapter MyD88 (Dinarello, 2009). A consequent phospho-signalling cascade activates NF- κ B leading to multiple effects on immunity including cytokine secretion, upregulation of adhesion and/or MHC/costimulatory molecules, increased vascular permeability, T_H17 cell differentiation, and effector T-cell proliferation in the presence of regulatory T cells (Sims & Smith, 2010). These powerful actions of IL-1 are countered by a receptor antagonist (IL-1RA), a decoy receptor (IL-1R2), and production of IL-1 α and IL-1 β as pro-proteins that require cleavage for full biological activity. IL-1 α is canonically cleaved by calpain, which occurs upon necrosis in some cell types and significantly increases activity (Burzynski, Humphry, Bennett, & Clarke, 2015; Zheng, Humphry, Maguire, Bennett, & Clarke, 2013), whilst IL-1 β is activated by caspase-1 (Black et al., 1988) after inflammasome engagement (Martinon, Burns, & Tschopp, 2002). How IL-1 α is released without necrosis is unknown and puzzling since IL-1 α release is inhibited in *Casp1*^{-/-} mice (Kuida et al., 1995; Li et al., 1995), even though IL-1 α is not a caspase-1 substrate. However, the original *Casp1*^{-/-} mice have an inactivating passenger mutation in *Casp11* (Kayagaki et al., 2011), suggesting caspase-11 might activate IL-1 α . Murine caspase-11 and the human orthologues caspase-4 and -5 are required for non-canonical inflammasome activation in response to intracellular LPS (icLPS) from bacterial infection (Kayagaki et al., 2011; Shi et al., 2014), and control monocyte IL-1 release (Vigano et al., 2015). Direct binding of LPS to caspase-11, -4 or -5 leads to pyroptosis and/or NLRP3 inflammasome activation, with IL-1 β and/or IL-1 α release (Kayagaki et al., 2011; Shi et al., 2014). However, whether caspase-4/5 or -11 require caspase-1 to mediate IL-1 α activation, if IL-1 α is only passively released, or if caspase-4/5 or -11 can directly cleave and activate IL-1 α in any of these systems is unknown.

We show that IL-1 α is specifically cleaved and activated at a conserved site by caspase-5 and -11, but not caspase-4. Knockdown of caspase-5 or expression of a caspase site mutant reduces release of IL-1 α after icLPS stimulation. IL-1 α cleavage and release from murine macrophages after icLPS requires only caspase-11, while IL-1 β needs both caspase-11 and -1. Importantly, we show caspase-5 and -11 are required for senescent cells to establish the IL-1 α -dependent SASP. Thus, IL-1 α is a direct substrate for inflammatory caspases during non-canonical inflammasome activation and senescence.

RESULTS

Caspase-5 cleavage of human IL-1 α at a conserved site increases activity.

Although non-canonical inflammasomes that utilise caspase-4 and -5 result in IL-1 α and/or IL-1 β release (Kayagaki et al., 2011; Shi et al., 2014), their role in cleavage or secretion of IL-1 α is unknown. Thus, we investigated whether IL-1 α could be proteolytically activated by these caspases. Incubation of recombinant pro-IL-1 α with active inflammatory caspases revealed that caspase-5 cleaved IL-1 α to a ~19kDa fragment, whilst caspase-1 or -4 did not (Fig. 1a), resulting in increased IL-1 α -specific cytokine activity (Fig. 1b). Both cleavage and increased IL-1 α activity was dependent on caspase-5 proteolytic activity, as the inhibitor LEVD-fmk reduced both (Fig. 1c,d). Caspases require Asp before the cleavage site, and thus important substrates show Asp conservation between species. Aligned IL-1 α protein sequences revealed a conserved IAND tetrapeptide motif (Fig. 1e), a known target of granzyme B (Afonina et al., 2011), with the Asp present in 81% of all sequences available (Ensembl). Cleavage at D¹⁰³ would produce a ~19kDa C-terminal fragment, which is congruent with the size seen by western (Fig. 1a). Mutation of Asp¹⁰³ to Ala abolished caspase-5 cleavage of pro-IL-1 α (Fig. 1f) and thus prevented activation (Fig. 1g). This shows that caspase-5 increases IL-1 α activity by direct processing at a conserved site located adjacent to the calpain site (Fig. 1h).

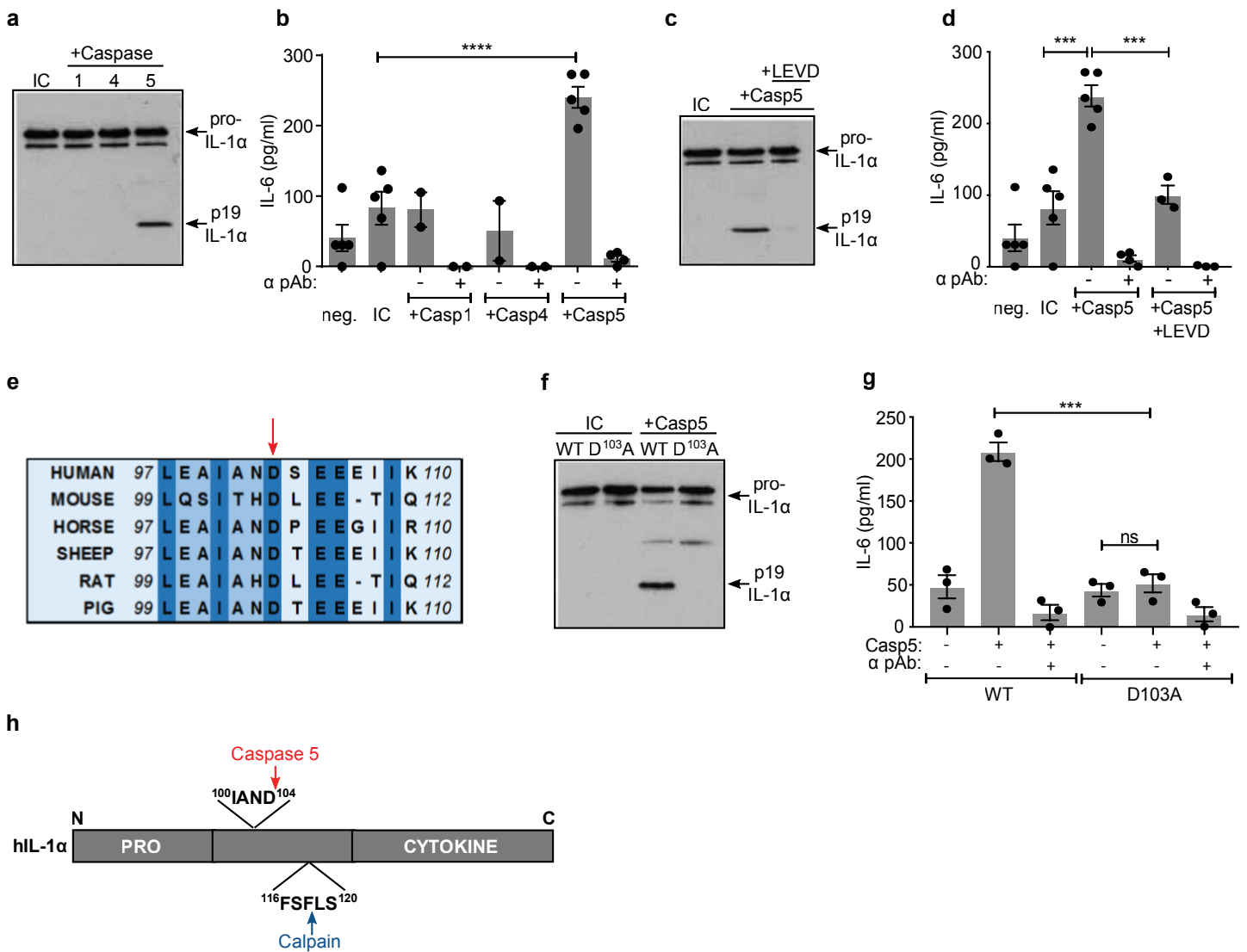


Figure 1: Caspase-5 cleavage of human IL-1α at a conserved site increases activity.

(a) Western blot for IL-1α after incubation of pro-IL-1α with active caspases, or alone (incubation control; IC). (b) IL-1-dependent IL-6 production by HeLa cells treated with reaction products from pro-IL-1α incubated ± active caspases, ± neutralising IL-1α antibody (α pAb). (c,d) Western blot (c) and bioactivity (d) of IL-1α after incubation ± caspase-5, ± caspase inhibitor LEVD. (e) Multi species IL-1α protein alignment showing conserved aspartic acid residue (arrow). (f) Western blot for wild-type (WT) or mutant D103A pro-IL-1α after incubation ± caspase-5, or alone (IC). (g) IL-1-dependent IL-6 production by HeLa cells treated with reaction products from WT or mutant pro-IL-1α incubated ± caspase-5, ± neutralising IL-1α antibody (α pAb). (h) Pictograph showing position of cleavage sites in IL-1α. Data represent mean ± s.e.m. of n = 3 (g), n = 4 (b,d); p = **≤0.01, ***≤0.001, ****≤0.0001; ns = not significant.

Release of cleaved IL-1 α from human cells requires caspase-5.

Due to the similar size of calpain and caspase-5 cleaved IL-1 α we produced a peptide antibody that was reactive to the region between the calpain and caspase-5 sites (Supplementary Fig. 1a) and developed an ELISA that recognised caspase-5 cleaved IL-1 α , but not pro-IL-1 α or calpain cleaved IL-1 α (Fig. 2a & Supplementary Fig. 1b). We also established an IL-1 α ELISA that recognised total cleaved IL-1 α , but not pro-IL-1 α (Supplementary Fig. 1c). To test IL-1 α processing and release in cells we expressed pro-caspase-5 and either wild-type (WT) or D¹⁰³A mutant pro-IL-1 α in HeLa cells, and transfected LPS into the cytosol (icLPS) to activate the non-canonical inflammasome. D¹⁰³A transfected cells released less total cleaved (Fig. 2b) and less non-calpain cleaved IL-1 α (Fig. 2c). Calpain cleaved D¹⁰³A equivalently to WT pro-IL-1 α (Fig. 2d), showing the mutation only prevents non-canonical processing. Furthermore, HeLa cells expressing WT pro-IL-1 α produced a 19 kDa IL-1 α fragment that was absent in D¹⁰³A expressing cells after icLPS (Fig. 2e). Primary human monocyte-derived macrophages (hMDMs) primed and then non-canonically activated with icLPS released non-calpain cleaved IL-1 α (Fig. 2f). Surprisingly, LPS/ATP activated hMDMs also produced non-calpain cleaved IL-1 α (Fig. 2g), suggesting caspase-5 may also cleave some pro-IL-1 α after canonical stimulation, likely due to the late activation of caspase-11 by caspase-1 (Kayagaki et al., 2011). Importantly, knockdown of caspase-5 in hMDMs (Fig. 2h) resulted in decreased release of total cleaved (Fig. 2i) and non-calpain cleaved IL-1 α (Fig. 2j) after icLPS treatment. This suggests that caspase-5 can directly process IL-1 α in cells, which results in increased activity and its subsequent release.

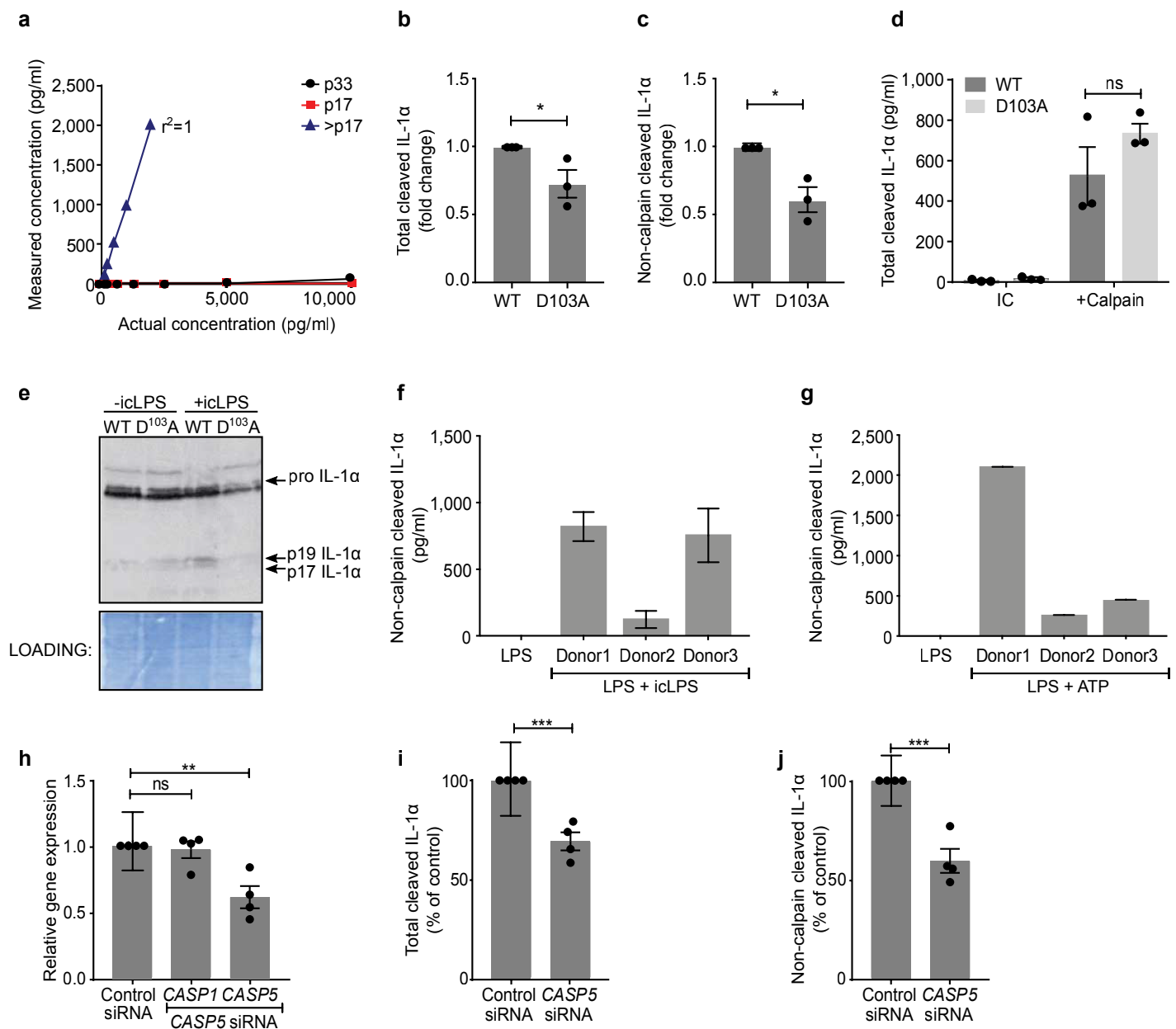


Figure 2: Release of cleaved IL-1 α from human cells requires caspase-5.

(a-d) ELISA data showing detection of recombinant pro (p33), calpain cleaved (p17), or non-calpain cleaved (>p17) IL-1 α (a), the level of total cleaved IL-1 α (b) or non-calpain cleaved IL-1 α (c) in the conditioned media of HeLa cells transfected with WT or D103A pro-IL-1 α and treated with intracellular LPS (icLPS), or total cleavage of WT or D103A pro-IL-1 α by calpain (d). (e) Western blot for IL-1 α in HeLa cells transfected with WT or D103A pro-IL-1 α , \pm icLPS treatment. (f,g) ELISA data showing level of non-calpain cleaved IL-1 α in the conditioned media of LPS primed human monocyte-derived macrophages (hMDMs) after icLPS (f) or ATP (g) treatment. (h) qPCR data showing relative gene expression in hMDMs after transfection of control or CASP5-targeted siRNA. (i,j) ELISA data showing level of total cleaved IL-1 α (i) or non-calpain cleaved IL-1 α (j) in the conditioned media of icLPS treated hMDMs after transfection of control or CASP5-targeted siRNA. Data represent mean \pm s.e.m. of $n = 3$ (b-d), $n = 4$ (h-j), or mean \pm s.d. of $n = 3$ separate donors (f,g); $p = * \leq 0.05$, $** \leq 0.01$, $*** \leq 0.001$; ns = not significant.

Release of cleaved IL-1 α from murine macrophages requires caspase-11.

Caspase-11 is the murine orthologue of human caspase-4 and -5, with all directly binding icLPS (Kayagaki et al., 2013; Shi et al., 2014), signifying functional conservation. Although caspase-4 is constitutively expressed (Kajiwara et al., 2014), only caspase-5 (Fig. 3a) and -11 (Fig. 3b) are upregulated by LPS, suggesting greater functional equivalence between caspase-5 and -11. Murine caspase-1 did not process (Fig. 3c) or activate (Fig. 3d) murine IL-1 α , while IL-1 β was cleaved and activated (Supplementary Fig. 2a,b), confirming murine IL-1 α is not a caspase-1 substrate. However, caspase-11 cleaved murine pro-IL-1 α at the conserved D¹⁰⁶ site (Fig. 3e), again increasing activity (Fig. 3f). Utilising bone marrow-derived macrophages (BMDMs) from WT, *Casp11*^{-/-}, and *Casp1*^{-/-}/*Casp11* transgenic (Tg) mice showed total loss of cleaved IL-1 α (Fig. 3g) and IL-1 β (Fig. 3h) secretion by *Casp11*^{-/-} BMDMs, as expected (Kayagaki et al., 2011). Importantly, release of cleaved IL-1 α was reinstated in *Casp1*^{-/-}/*Casp11*^{Tg} BMDMs (Fig. 3i), suggesting IL-1 α only requires caspase-11 for cleavage and release after icLPS. The reason *Casp1*^{-/-}/*Casp11*^{Tg} BMDMs do not release WT levels of IL-1 α is thought to be due to incomplete complementation of endogenous *Casp11* by the *Casp11* transgene, as shown previously (Kayagaki et al., 2011). Interestingly, *Casp1*^{-/-}/*Casp11*^{Tg} BMDMs did not release IL-1 β (Fig. 3j), showing IL-1 β requires both caspase-1 and -11. To determine if caspase-11 processing of pro-IL-1 α drives IL-1 α release, as opposed to passive leakage after caspase-11-induced cell lysis, we expressed low levels of WT or D¹⁰⁶A murine pro-IL-1 α in immortalised mBMDMs, and treated with icLPS. Expression of WT IL-1 α significantly increased release of cleaved IL-1 α , while D¹⁰⁶A mutant expressing macrophages released the same amount of cleaved IL-1 α as empty vector transfected cells (Fig. 3k). Importantly, no difference in viability (Supplementary Fig. 3a,b) or IL-1 β release after icLPS was seen between groups (Fig. 3l), indicating effect on IL-1 α only. Together, these data show that caspase-11 cleavage of murine IL-1 α at D¹⁰⁶A is required for full activity and release from murine macrophages, while IL-1 β activation and release still requires caspase-1 and -11.

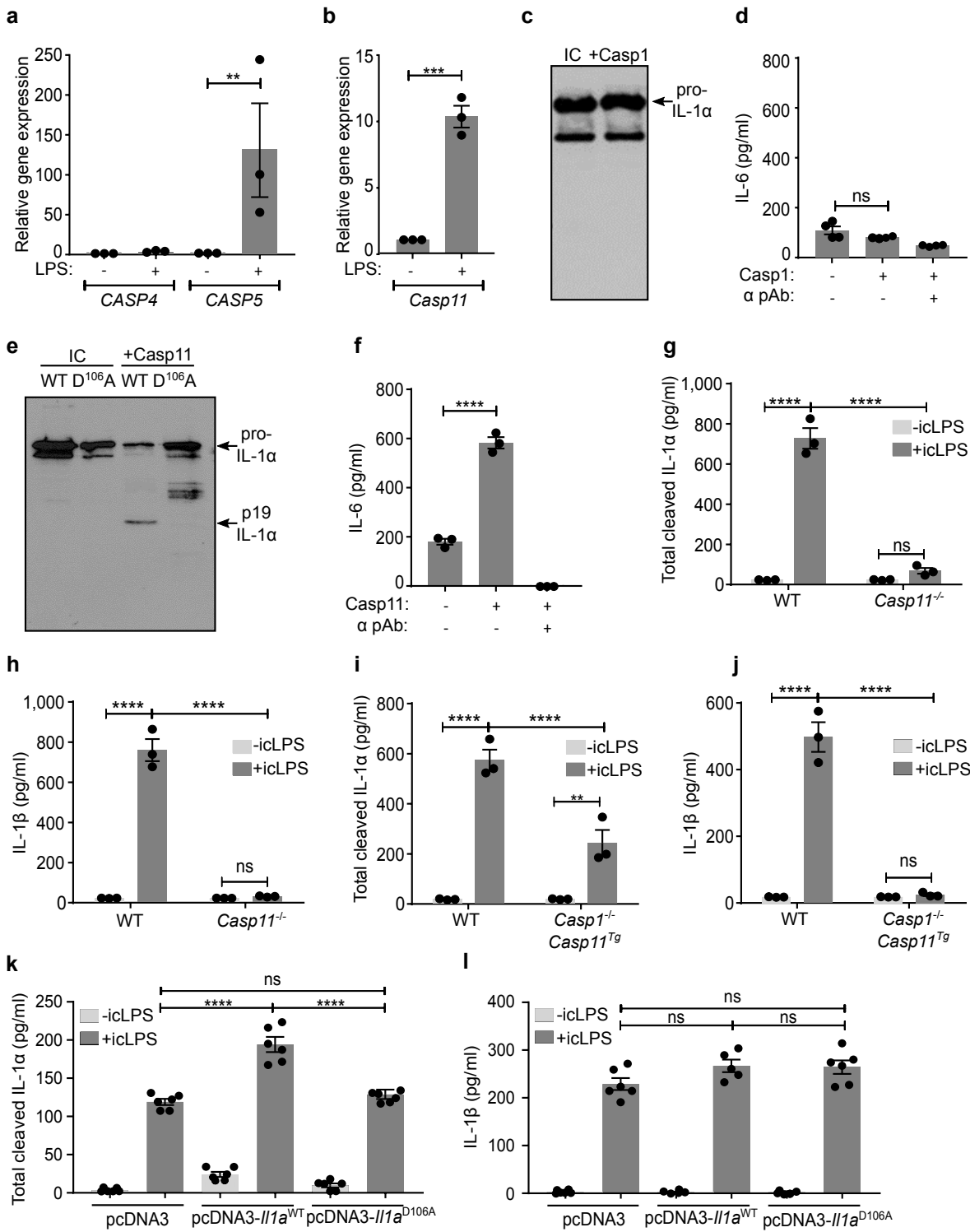


Figure 3: Release of cleaved IL-1 α from murine macrophages requires caspase-11.

(a,b) qPCR data showing changes in *CASP4*, *CASP5* (a) or *Casp11* (b) transcript after LPS treatment of primary human (a) or mouse (b) macrophages. (c) Western blot for IL-1 α after incubation of murine pro-IL-1 α with murine caspase-1, or alone (IC). (d) IL-1-dependent IL-6 production by murine fibroblasts treated with reaction products from murine pro-IL-1 α incubated \pm murine caspase-1. (e,f) Western blot of murine wild-type (WT) or D106A pro-IL-1 α (e) and bioactivity of murine WT pro-IL-1 α (f) after incubation \pm caspase-11. (g-l) ELISA data showing the level of cleaved IL-1 α (g,i,k) or IL-1 β (h,j,l) detected in the conditioned media of: mouse bone marrow-derived macrophages (mBMDMs) from WT, *Casp11*^{-/-} (g,h) or *Casp1*^{-/-}*Casp11*^{Tg} (i,j) mice, or immortalised mBMDMs transfected with empty, WT *Il1a* or D106A *Il1a* vectors (k,l), followed by LPS priming and then transfection of intracellular LPS (icLPS). Data represent mean \pm s.e.m. of n = 3 (a,b,f-l), n = 4 (d); p = ** \leq 0.01, **** \leq 0.0001, ***** \leq 0.00001; ns = not significant.

Caspase-5 is required for the IL-1 α -dependent senescent-associated secretory phenotype.

The SASP directs clearance of senescent cells, but also drives chronic inflammation that can promote disease and unhealthy aging. As IL-1 α drives the SASP we investigated whether caspase-5 is required for IL-1 α release during senescence. We utilised the well-characterised tamoxifen-inducible HRAS^{G12V}-induced senescence of human IMR-90 fibroblasts. Seven days after tamoxifen cultures were positive for senescence-associated beta galactosidase (SA β G) (Fig. 4a), had reduced proliferation (Fig. 4b), and showed senescence-associated heterochromatic foci (SAHF) (Fig. 4c). Senescent cultures showed increased expression of *CASP5* (Fig. 4d), cell surface IL-1 α (Fig. 4e & Supplementary Fig. 4), and total cleaved IL-1 α in the conditioned media (Fig. 4f), compared to growing cells. Importantly, similar low levels of death were found in growing and senescent cultures (Fig. 4g), excluding passive release of IL-1 α after cell lysis. Senescent cells released the common SASP cytokines IL-6 (Fig. 4h), IL-8 and MCP-1 (Supplementary Fig. 5), which were all dependent on IL-1 α . Consistent with this, although pro-IL-1 β was upregulated in senescent cells, negligible amounts were cleaved to the mature form and none was released from the cell (Supplementary Fig. 6a,b). siRNA-mediated knockdown of *CASP5* (Fig. 4i) led to significantly less cell surface IL-1 α (Fig. 4j & Supplementary Fig. 4), reduced release of total (Fig. 4k) and non-calpain cleaved (Fig. 4l) IL-1 α , and a subsequent reduction in IL-6, IL-8 and MCP-1 (Fig. 4m-o). Caspase-5 was also required for the SASP in WI-38 cells (Supplementary Fig. 7a-e). With either cell type, *CASP5* knockdown did not alter SA β G or proliferation levels (Supplementary Fig. 8a,b). The SASP is dependent on cGAS sensing of cytosolic chromatin, which drives interferon signalling (Gluck et al., 2017; Yang, Wang, Ren, Chen, & Chen, 2017). As *CASP5* is interferon responsive, we tested if its expression was cGAS-dependent. *cGAS* knockdown resulted in reduced release of IL-1 α and IL-6, as expected, but also decreased *CASP5* expression (Supplementary Fig. 9a-d). Together, this suggests that release of cleaved fully active IL-1 α and expression of the subsequent SASP is dependent on caspase-5, with upstream cGAS potentially controlling *CASP5* expression.

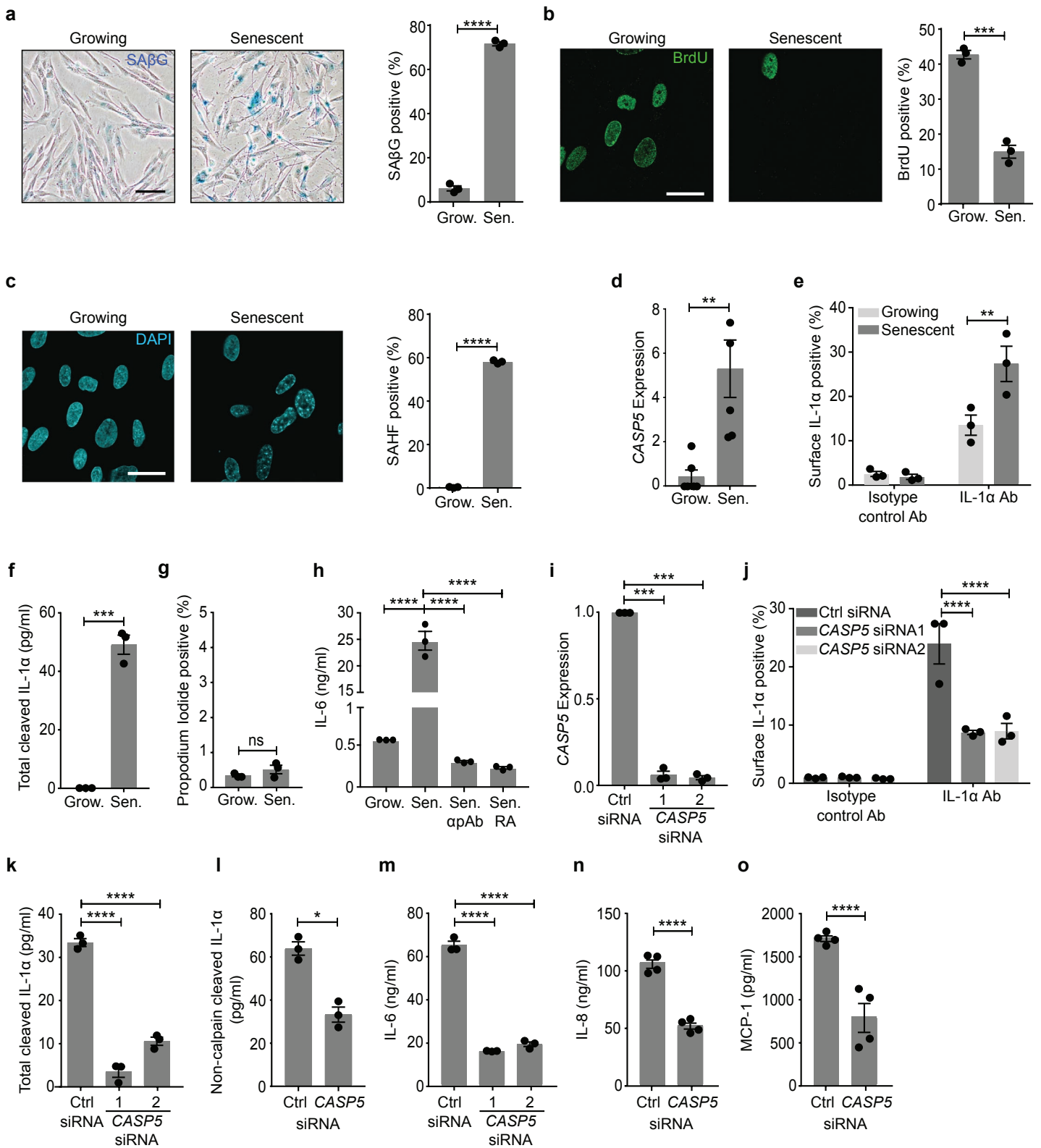


Figure 4: Caspase-5 is required for the IL-1 α -dependent SASP.

(a-c) Representative images and quantification of senescence-associated beta galactosidase (SA β G) (a), proliferation by BrdU (b), and senescence-associated heterochromatic foci (SAHF) (c) in growing (Grow.) and senescent (Sen.) IMR-90 cells (n.b. b,c are the same field of view). (d-g) Caspase-5 expression by RNA-Seq (d), cell surface IL-1 α by flow cytometry (e), cleaved IL-1 α in the conditioned media by ELISA (f), and level of cell death (g) in growing and senescent IMR-90 cells. (h) ELISA data showing the level of IL-6, \pm neutralising IL-1 α antibody (α pAb) or IL-1RA (RA) in the conditioned media of growing and senescent IMR-90 cells. (i) qPCR data showing relative expression of CASP5 in senescent IMR-90 cells after transfection of control (Ctrl) or CASP5-targeted siRNAs. (j-o) Cell surface IL-1 α by flow cytometry (j), or total cleaved IL-1 α (k), non-calpain cleaved IL-1 α (l), IL-6 (m), IL-8 (n) and MCP-1 (o) by ELISA in the conditioned media of senescent IMR-90 cells after transfection of control or CASP5-targeted siRNA. Data represent mean \pm s.e.m. of n = 3, n = 4 (n,o), n = 6 (d); p = * \leq 0.05, ** \leq 0.01, *** \leq 0.001, **** \leq 0.0001; ns = not significant. Scale bars = 100 μ m (a), 15 μ m (b,c).

Caspase-11 is required for immune surveillance of senescent cells *in vivo*.

To investigate if caspase-11 is required for the SASP *in vivo* we used a mouse liver model of NRAS-induced senescence. Using hydrodynamic tail vein injection we delivered *Nras*-IRES-*Casp11* shRNA or *Nras*-IRES-Control shRNA constructs that undergo transposon-mediated stable integration into hepatocytes (T. W. Kang et al., 2011). This system was chosen as it decreases caspase-11 in only senescent cells, as opposed to all cells in *Casp11*^{-/-} mice. Caspase-11 protein was increased in NRAS positive cells after control shRNA treatment (Fig. 5a), with ~97% of cells co-staining for NRAS and caspase-11 (Fig. 5b), while reduced caspase-11 protein (Fig. 5c,d) and transcript (Fig. 5e) was seen with the *Casp11*-targeted construct. This indicates that caspase-11 is upregulated during NRAS-induced hepatocyte senescence *in vivo* and that *Casp11*-targeted shRNA reduces expression. No difference in the number of NRAS positive cells between control- or *Casp11*-targeted shRNA was seen at day 3, indicating equivalent integration and subsequent induction of senescence by NRAS (Fig. 5f,g). However, *Casp11* knockdown caused a significant accumulation of NRAS positive cells at days 6 and 12 (Fig. 5f,g), and a significant negative correlation existed between the level of caspase-11 and number of NRAS positive cells within livers (Supplementary Fig. 10), indicative of a reduction in SASP-driven immune-mediated clearance. Consistent with this, the number of early infiltrating macrophages was decreased with *Casp11* knockdown (Fig. 5h), along with the number of immune cells clustering around NRAS positive cells (Supplementary Fig. 11a,b). Importantly, the number of Ki67/NRAS double positive cells was equivalent between groups (Fig 5i), eliminating the possibility that accumulation of NRAS positive cells was due to *Casp11* knockdown causing bypass of senescence. Together, this suggests that establishment of the IL-1 α -dependent SASP that drives immune surveillance and clearance is dependent on caspase-11 *in vivo*.

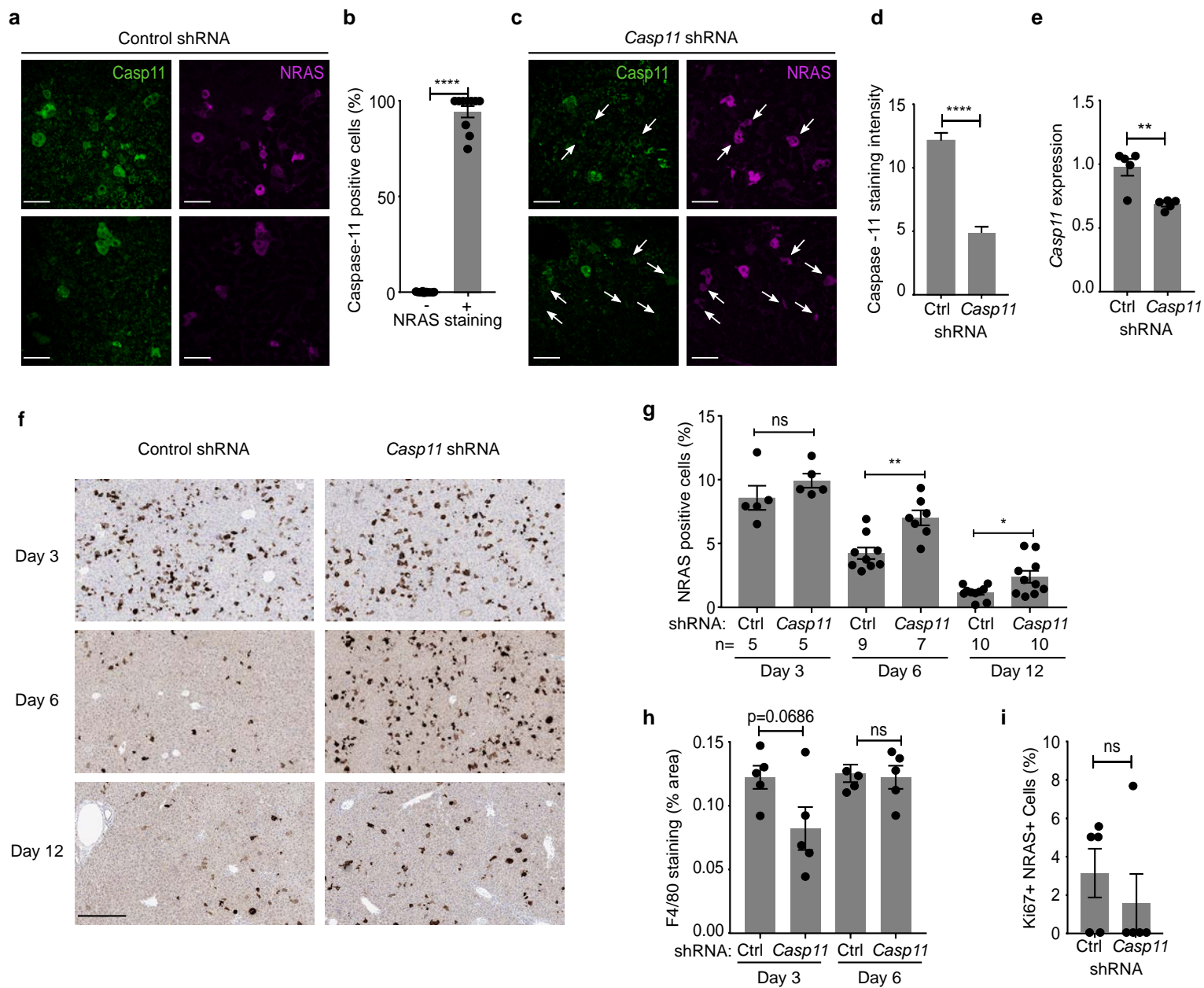
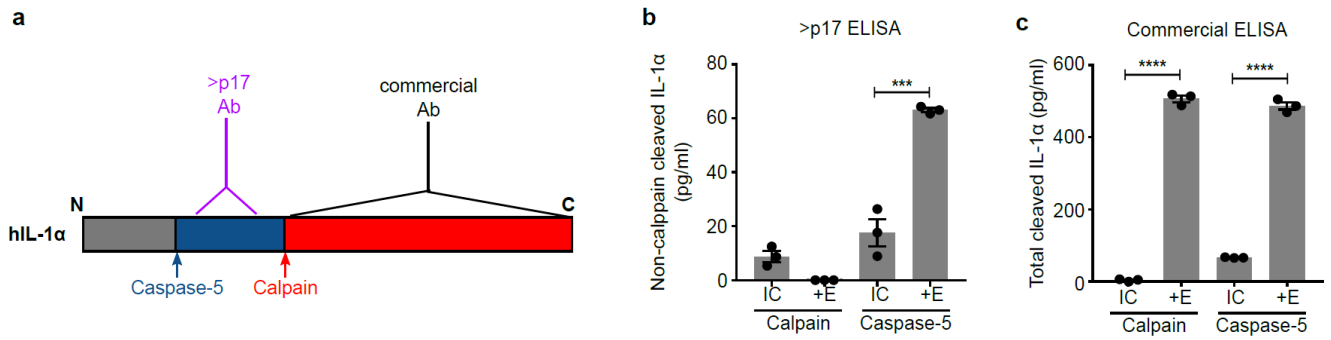
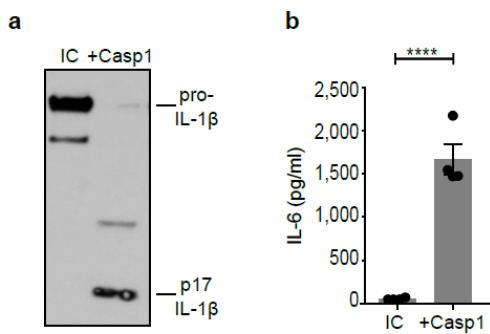


Figure 5: Caspase-11 is required for immune surveillance of senescent cells *in vivo*.

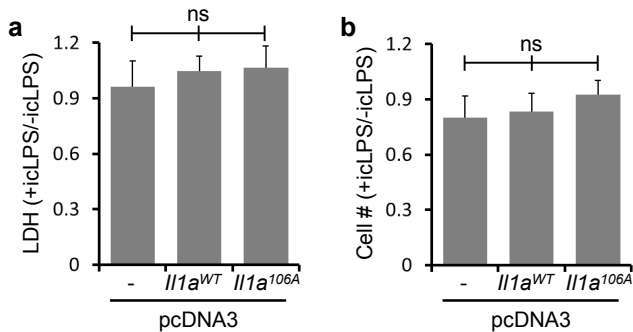
(a-d) Representative images (a,c) and quantification (b,d) of caspase-11 (green) and RAS (magenta) staining in individual liver cells 6 days after hydrodynamic tail vein injection of NRAS with control (a,b) or *Casp11*-targeted (c,d) shRNA constructs. White arrows indicate RAS+ve/caspase-11 -ve cells (c). (e) qPCR data showing the level of *Casp11* expression in livers 3 days after injection of constructs as indicated. (f,g) Representative images (f) and quantification (g) of NRAS staining (brown) in livers after the time and injection of constructs as indicated. (h) Quantification of F4/80 staining in livers treated as indicated. (i) Quantification of number of Ki67/NRAS double +ve cells in livers 6 days after injection of constructs. Data represent mean \pm s.e.m. of n = 5 (b,d,e,h,i), or as indicated (g). p = * \leq 0.05, ** \leq 0.01, **** \leq 0.0001; ns = not significant. Scale bars = 50 μ m (a,c), 300 μ m (f).



Supplementary Figure 1: (a) Schematic showing location of the custom peptide antibody relative to the calpain and caspase-5 cleavage sites in pro-IL-1 α . (b-c) Data showing specificity of our custom non-calpain cleaved IL-1 α ELISA (b) or a total cleaved IL-1 α ELISA (c) for detecting either calpain or caspase-5 cleaved pro-IL-1 α . IC = incubation control (no enzyme); +E = +enzyme. Data represent mean \pm s.e.m. of n = 3; p= **** \leq 0.001, ***** \leq 0.0001.



Supplementary Figure 2: (a) Western blot for IL-1 β after incubation of murine pro-IL-1 β with murine caspase-1, or alone (IC). (b) IL-1-dependent IL-6 production by murine fibroblasts treated with reaction products from murine pro-IL-1 β incubated \pm murine caspase-1. Data represent mean \pm s.e.m. of n = 4; p= **** \leq 0.0001.

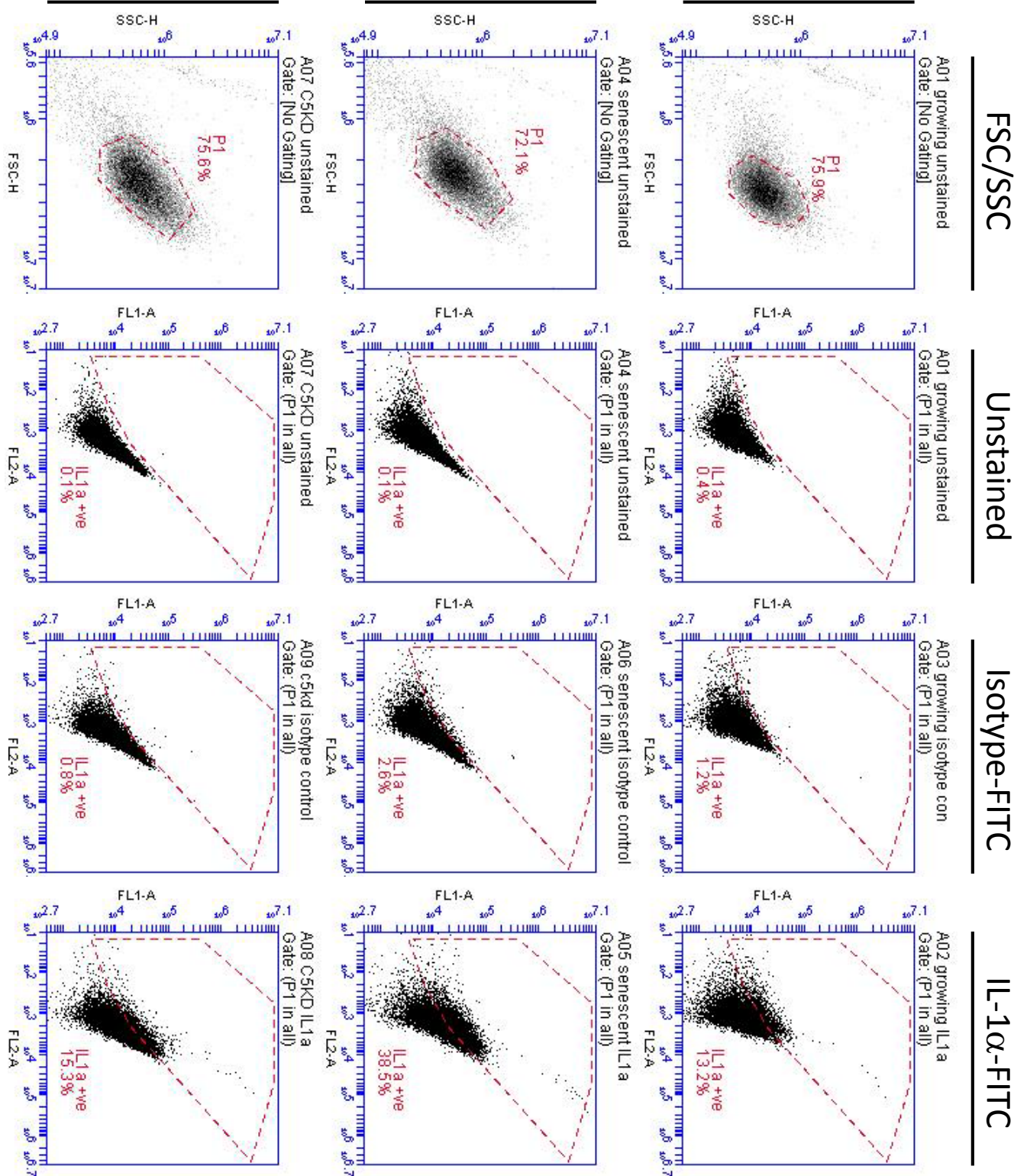


Supplementary Figure 3: (a,b) Analysis of cell viability by release of lactate dehydrogenase (LDH) into the conditioned media (a) and number of cells attached by crystal violet staining (b) in immortalised mBMDMs after transfection of empty, WT *Il1a* or D106A *Il1a* vectors, followed by LPS priming and then transfection of intracellular LPS (icLPS). Data represent mean \pm s.d. of n = 3; ns = not significant.

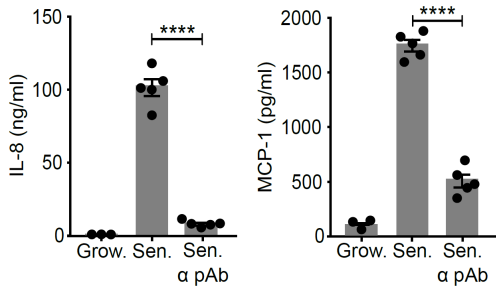
Senescent
+*CASP5* KD

Senescent

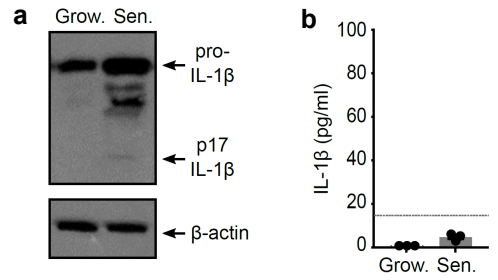
Growing



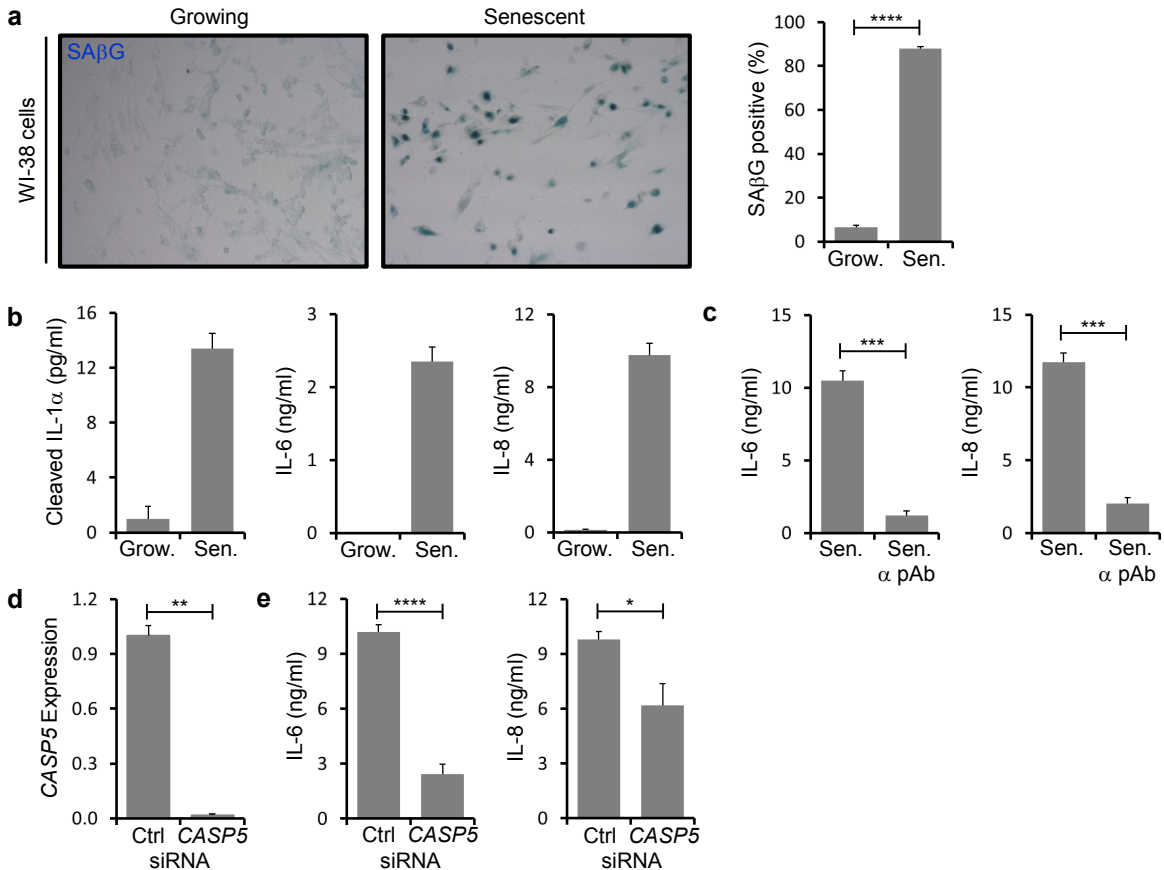
Supplementary Figure 4: Representative flow cytometry dot plots of growing IMR-90 cells, senescent IMR-90 cells and senescent IMR-90 cells after *CASP5* knockdown, which were left unstained or stained with isotype control-FITC or anti-IL-1 α -FITC antibodies before analysis by flow cytometry.



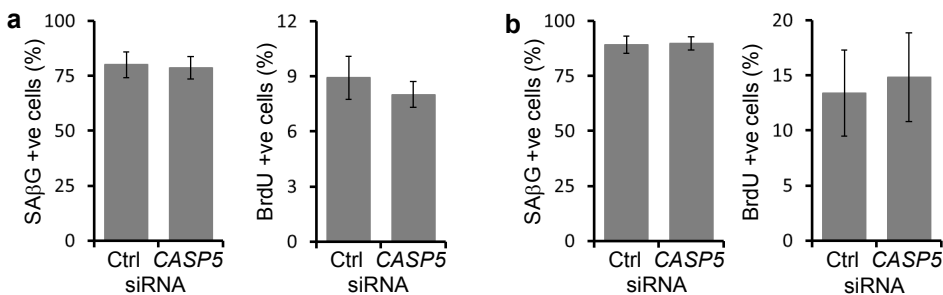
Supplementary Figure 5: ELISA data showing the level of IL-8 and MCP-1 in the conditioned media of growing (Grow.) or senescent (Sen.) IMR-90 cells, ± neutralising IL-1 α antibody (α pAb). Data represent mean \pm s.e.m. of $n \geq 3$; $p = **** \leq 0.0001$.



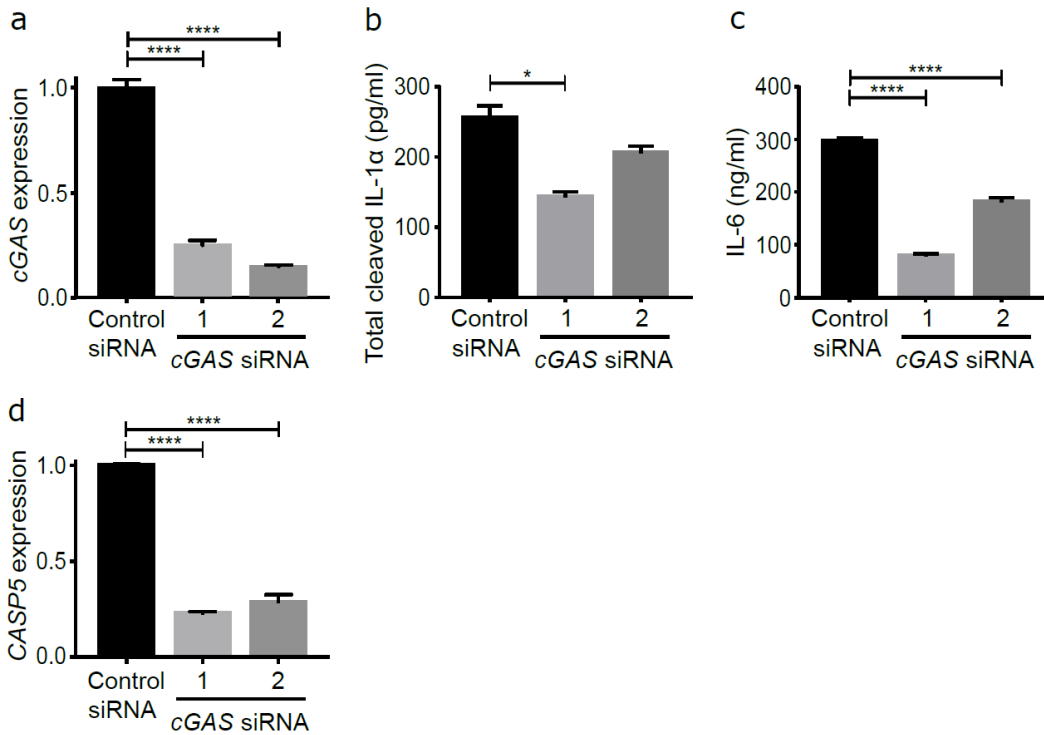
Supplementary Figure 6: (a) Western blot for IL-1 β in growing (Grow.) and senescent (Sen.) IMR-90 cells. (b) ELISA data showing the level of IL-1 β in the conditioned media of growing and senescent IMR-90 cells. Grey dotted line indicates limit of detection. Data represent mean \pm s.e.m. of $n = 3$.



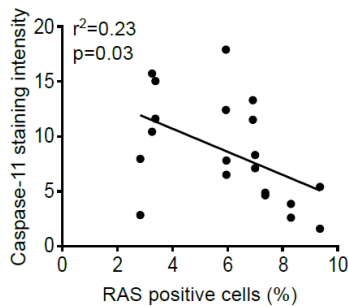
Supplementary Figure 7: (a) Representative images and quantification of senescence-associated beta galactosidase (SA β G) staining in growing (Grow.) and senescent (Sen.) WI-38 cells. (b,c) ELISA data showing the level of cleaved IL-1 α and/or SASP factors in the conditioned media of growing and senescent WI-38 cells (b), or senescent WI-38 cells ± neutralising IL-1 α antibody (α pAb) (c). (d,e) Relative CASP5 expression by qPCR (d) or SASP factors in the conditioned media by ELISA (e) in senescent WI-38 cells after transfection of control (Ctrl) or CASP5-targeted siRNA. Data represent mean \pm s.e.m. of $n \geq 3$ (a,c-e); or mean \pm s.d. of $n=2$ (b); $p = * \leq 0.05$, $** \leq 0.01$, $*** \leq 0.001$, $**** \leq 0.0001$.



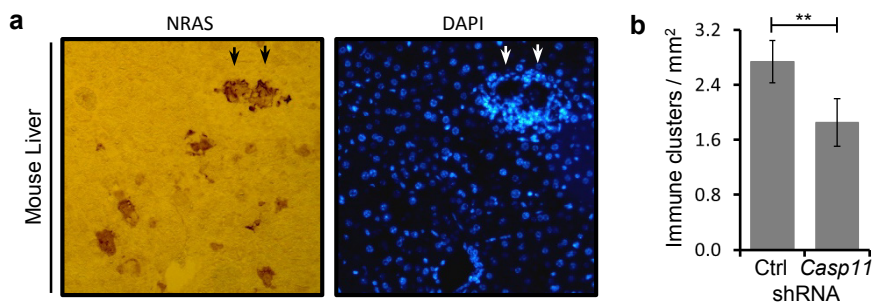
Supplementary Figure 8: (a,b) Level of SA β G and BrdU +ve cells in senescent IMR-90 (a) and WI-38 (b) cell cultures after transfection of control (Ctrl) or CASP5-targeted siRNAs. Data represent mean \pm s.d. representative of $n = 2$.



Supplementary Figure 9: (a) qPCR data showing relative expression of cGAS in senescent IMR-90 cells after transfection of control or cGAS-targeted siRNAs. (b-d) Total cleaved IL-1 α (b) and IL-6 (c) by ELISA in the conditioned media, or CASP5 expression by qPCR (d) in senescent IMR-90 cells after transfection of control or cGAS-targeted siRNAs. Data represent mean \pm s.e.m. of $n = 3$ (a-c), $n = 6$ (d); $p = * \leq 0.05$, **** ≤ 0.0001 .



Supplementary Figure 10: Linear regression analysis of the correlation between average caspase-11 staining intensity and percentage of RAS positive cells in mouse livers 6 days after injection.



Supplementary Figure 11: (a) Representative images of immune cells clustering around two NRAS⁺ senescent cells (arrows) within mouse liver 6 days after hydrodynamic tail vein injection of NRAS. (b) Quantification of immune cell clusters around NRAS⁺ cells within mouse liver 6 days after hydrodynamic tail vein injection of NRAS with control (Ctrl) or *Casp11*-targeted shRNA constructs. Data represent mean \pm s.d. of $n = 5$ mice; $p = ** \leq 0.01$.

DISCUSSION

Due to the powerful, pleiotropic effects of IL-1, unprecedented levels of control and feedback pathways are required to mount an immune response that resolves an insult without causing overt tissue damage. For example, multiple inflammasomes have evolved to distinguish tissue damage, environmental pollutants, bacteria, viruses, fungi and protozoa. IL-1 also drives homeostatic processes such as thermoregulation (Dinarello, 2009), regulatory B cell differentiation (Rosser et al., 2014), intestinal integrity (Jung et al., 2015), and the immune surveillance and clearance of senescence cells (T. W. Kang et al., 2011). However, how IL-1 α is cleaved, activated and released was unknown.

We find that IL-1 α is directly cleaved by caspase-5 and -11 at a conserved site, leading to full cytokine activity. Expression of a caspase site mutant IL-1 α or knockdown of *CASP5* prevents release of cleaved IL-1 α from cells, while IL-1 α cleavage and release from murine macrophages requires only caspase-11, with IL-1 β needing both caspase-11 and -1. Importantly, the IL-1 α -dependent SASP requires caspase-5 and -11 in vitro and in vivo. Thus, IL-1 α is a direct substrate of inflammatory caspases during non-canonical inflammasome activation and senescence.

The original *Casp1*^{-/-} mice (Kuida et al., 1995; Li et al., 1995) showed loss of IL-1 β release from macrophages and during endotoxaemia. Unexpected reduced levels of IL-1 α were also found, which has remained a puzzle as IL-1 α is not a caspase-1 substrate. However, *Casp1*^{-/-} mice inherited a *Casp11* inactivating passenger mutation from the 129/Sv background (Kayagaki et al., 2011). Our data suggest that defective release of cleaved IL-1 α in *Casp1*^{-/-} mice is likely due to the absence of caspase-11. Indeed, serum levels of cleaved IL-1 α are undetectable during endotoxaemia (which activates non-canonical inflammasomes via caspase-11) in *Casp11*^{-/-} and *Casp1*^{-/-}/*Casp11*^{-/-} mice, yet restored in the *Casp1*^{-/-}/*Casp11*^{Tg} (Kayagaki et al., 2011), supporting this concept. The primary role of caspase-4/5 and -11 is thought to be LPS binding, and few substrates known. Gasdermin D is shown to be a key substrate for caspase-11, -4/5 and indeed caspase-1 (Kayagaki et al., 2015; Shi et al., 2015). We now report IL-1 α as a direct substrate for caspase-5 and -11.

Although independent publications show cleavage of IL-1 α greatly increases activity (Afonina et al., 2011; Zheng et al., 2013), others contest this (Kim et al., 2013). Kim *et al* purified pro-IL-1 α by HPLC, which typically denatures proteins due to the organic solvent mobile phase, and we find denatured and refolded pro-IL-1 α has more activity than native pro-IL-1 α (Zheng et al., 2013). Regardless, how IL-1 α is released and if cleavage is required was unknown. Gasdermin D-mediated pore formation can allow IL-1 α to exit cells (Kayagaki et al., 2015; Shi et al., 2015). However, because all tested IL-1 α ELISA kits only recognise the cleaved form (KW, MH, MC unpublished), detection of IL-1 α within conditioned media represents both release and cleavage. Thus, active caspase-5 or -11 could drive both the direct processing of IL-1 α and release via gasdermin-D pores. In addition, pro-IL-1 α is bound to IL-1R2 inside many cells, which prevents activation by calpain (Burzynski et al., 2015; Zheng et al., 2013). However, caspase-1 can cleave IL-1R2 to enable IL-1 α activation, and this action may partly control canonical IL-1 α release (Zheng et al., 2013). Interestingly, caspase-5, but not caspase-4, also cleaves IL-1R2 (Zheng et al., 2013). After canonical stimuli (e.g. LPS/ATP) IL-1 α release is dependent on ASC and NLRP3 (Kayagaki et al., 2011), whilst non-canonical stimuli only require caspase-11 for cleaved IL-1 α release (Fig. 3i & (Kayagaki et al., 2011)). This suggests that canonical IL-1 α release could proceed via NLRP3 caspase-1 activation and cleavage of IL-1R2, followed by calpain cleavage of IL-1 α , whilst non-canonical pathways could lead to IL-1 α release after direct cleavage of IL-1R2 and IL-1 α by caspase-5/11.

In murine systems caspase-11 binds LPS, increases caspase-1 cleavage of IL-1 β (Wang et al., 1998), activates gasdermin-D (Kayagaki et al., 2015; Shi et al., 2015), and now also directly cleaves and activates IL-1 α . In humans an ancestral gene duplication resulted in *CASP4* and *CASP5*, with caspase-4 suggested as the closer homologue of caspase-11 (Shi et al., 2014). Both caspase-4 and -5 bind LPS and target gasdermin D, but only caspase-5 can complement *Casp11*^{-/-} cells (Shi et al., 2014), only *CASP5* and *Casp11* are upregulated in response to LPS (Fig. 3a,b), and only caspase-5/11 can cleave

IL-1 α , suggesting a closer functional connection. We suggest caspase-4 and -5 have most likely undergone subfunctionalisation, with functionality of the ancestral *Casp11*-like gene now distributed between both. However, if each performs non-redundant roles, and what these are, is still unknown.

Although IL-1 α induces sterile inflammation upon release from damaged cells it also drives the SASP, but in this context IL-1 α release or surface presentation occurs without cell death (Fig. 4g & (Gardner et al., 2015)). This excludes the usual notion that IL-1 α is passively released (Kayagaki et al., 2011). IL-1 α expression during the SASP is controlled in part by ATM/ATR liberation of GATA4 from p62-directed autophagy (C. Kang et al., 2015) and/or an mTORC1-dependent pathway (Laberge et al., 2015). Also, redox balance and Ca²⁺ levels may enhance calpain processing of IL-1 α in senescent cells (McCarthy, Clark, Bartling, Trebak, & Melendez, 2013). Thus, how active IL-1 α is released without cell death during senescence was unknown. Here we report increased *CASP5* or *Casp11* expression in senescent cells and a loss of cell surface and released IL-1 α without caspase-5, leading to inhibition of the SASP. Interestingly, the SASP is not dependent on IL-1 β (Gardner et al., 2015; Orjalo et al., 2009), implying cleaved IL-1 α release occurs separately from IL-1 β (e.g. without caspase-1/NLRP3/ASC), in contrast to other studies (Acosta et al., 2013). Indeed, IL-1 β release after icLPS requires caspase-1 and -11, whilst IL-1 α only requires caspase-11 (Fig. 3g-j). Together this suggests that cleavage of IL-1 α by caspase-5/11 during senescence leads to release of active IL-1 α only, which drives the SASP. Interestingly, *CASP5* mutations are associated with cancers (Offman et al., 2005), while *CASP1* and *CASP4* mutations are not (Soung et al., 2008), suggesting a caspase-5-specific protective role against tumorigenesis that is in keeping with SASP-driven senescence surveillance.

In conclusion, we show that IL-1 α is a direct substrate of the non-canonical inflammatory caspase-5 and -11, with cleavage increasing cytokine activity and release. Conservation of the cleavage site between species implies that activation of IL-1 α by caspase-5 or -11 is important. Indeed, cleavage of IL-1 α by caspase-5 or -11 is essential for the SASP. Thus, directly targeting caspase-5 may reduce inflammation and limit the deleterious effects of senescent cells that accumulate during disease and aging.

MATERIALS AND METHODS

All material from Sigma-Aldrich unless otherwise stated.

Cell Culture

HeLa cells (ECACC) and primary mouse fibroblasts were cultured in DMEM with penicillin, streptomycin, L-glutamine and 10% FCS and passaged at 80% confluency. IMR90 and WI-38 cells (ATCC) were cultured in phenol red free DMEM supplemented with penicillin, streptomycin and 10% FCS. Bone marrow derived macrophages (BMDMs) from wild-type, *Casp11*^{-/-} or *Casp1*^{-/-}*Casp11*^{Tg} (Kayagaki et al., 2011) mice (C57BL6/J background, 8-12 weeks old) were differentiated in RPMI 1640 with penicillin, streptomycin, L-glutamine, 10% FCS and 15% L929 conditioned media, while immortalised BMDMs used the same media, but without L929. Human monocyte-derived macrophages were isolated from whole blood (obtained with informed consent; NRES Committee, East of England) with percoll gradients and differentiated in Iscove's with streptomycin, L-glutamine and 10% autologous serum. IMR90 and WI-38 cells were transduced with retrovirus carrying ER:*HRAS*^{G12V} in pLNCX2 (Clontech), as previously described (Young et al., 2009), and senescence induced with 4-hydroxytamoxifen (100nM). All cells were checked for mycoplasma contamination (MycoAlert, Lonza). HeLa cells were transfected with pcDNA3 (Invitrogen) using Fugene HD (Promega), whilst immortalised mBMDMs used Amaxa nucleofection (Lonza), before incubation (48h, 37°C). Knockdown in primary macrophages was performed with 10pmol of non-targeting or *CASP5*-targeting siGENOME siRNA pool (Dharmacon), whilst knockdown in IMR90 and WI-38 cells was performed with 10pmol of pooled or individual *CASP5*-, or *cGAS*-targeting siGENOME siRNAs, using Lipofectamine RNAiMAX (Invitrogen) as per the manufacturer's instructions. Cell viability was assessed by LDH release (Pierce), or crystal violet staining as previously described (Gardner et al., 2015).

IL-1 Bioassays and Inflammasome Activation

HeLa cells or mouse fibroblasts were plated (10,000 cells/well, 48-well plate) and incubated (16h, 37°C). Media was refreshed and cells incubated (6h, 37°C) ± cleavage assay products (1.5µl). Specific IL-1 activity was inferred by the effect of neutralising antibodies (2µg/ml; same as for Westerns), on IL-6 production. Every experiment contained a media only negative control and a recombinant IL-1 (10ng/ml; Peprotech) positive control. For non-canonical, cells were primed with ultrapure LPS (1µg/ml, 4h; Invivogen) in full media, transfected with ultrapure LPS (5µg/ml) using Fugene HD (2.5µl/ml; Promega), and incubated in Optimem (37°C, 18h). For canonical, cells were primed with ultrapure LPS (1µg/ml, 4h) in full media, treated with ATP (5mM, pH7; Invivogen), and incubated in Optimem (37°C, 18h).

Recombinant Protein Expression, Purification and Cleavage

Pro-IL-1 α/β or pro-caspase-5 cDNAs were cloned into pGEX-4T-3 (GE) or pcDNA3 (Invitrogen), with mutations introduced by site-directed mutagenesis. For bacterial expression IPTG-induced Rosetta cultures were lysed (PBS 1x; DTT 1mM; EDTA 10mM; benzonase 30U/ml; lysozyme 55kU/g (both Novagen); protease inhibitor cocktail) with sonication, and clarified by centrifugation (5525 g, 1h, 4°C). Filtered supernatants were loaded onto a GStap column (GE), washed (PBS; DTT 1mM; EDTA 1mM) and eluted (Tris 50mM; NaCl 100mM; DTT 1mM; reduced L-Glutathione 50mM; adjusted to pH 8) using an ÄKTA FPLC system (GE). Eluted protein was dialysed overnight (Tris 10mM, pH8; NaCl 50mM) and stored in glycerol (10%) at -80°C. IL-1 protein concentration was normalised by SDS PAGE, coomassie staining (G-250; Biorad) and quantitative imaging (Odyssey, Li-Cor). Recombinant IL-1 (4µg/ml) was incubated (1h, 37°C) with active caspase (100U or 10U; all Enzo) in reaction buffer (Human - HEPES 50mM, pH 7.4; NaCl 100mM; CHAPS 0.1%; EDTA 1mM; glycerol 10%; DTT 10mM) (Mouse - MES 100mM, pH 6.5; CHAPS 0.1%; PEG 10%; DTT 10mM). Where indicated LEVD-FMK (330 µM; Enzo) was added. Recombinant IL-1 (4µg/ml) was incubated (1h, RT) with active calpain (100U; Calbiochem) in reaction buffer (NaCl 100mM; CaCl₂ 2mM; DTT 1mM).

Induction of mouse hepatocyte senescence in vivo

Mice were handled and kept under pathogen-free conditions in accordance with UK law and institutional guidelines at the University of Cambridge and CRUK Cambridge Institute. Transposon-mediated gene transfer by hydrodynamic tail vein injection was as previously described (Dauch et al., 2016; T. W. Kang et al., 2011). Briefly, short-hairpin oligomers targeting *Casp11* (5'-TACCATCTATCAGATATTCAA-3') were cloned into MSCV-miR30-puro before sub-cloning into pCaNIG-miR30 (from Lars Zender (Dauch et al., 2016)). Vectors were prepared using the EndoFree MaxiPrep Kit (Qiagen). Female C57BL/6 mice (Charles River) were injected via the lateral tail vein with pCaNIG-miR30 (20µg) and SB13 transposase vector (5µg) in PBS at a volume equivalent to 10% of body weight in less than 10 seconds, and livers harvested at the times indicated.

Western blotting and Cytokine Detection

Western blotting was performed as previously described. Blocked PVDF membranes (Biorad) were incubated (16h, 4°C) with: anti-human IL-1α (500-P21A, Peprotech; 1:500), anti-mouse IL-1α (AF-400NA, R&D; 1:500), anti-human IL-1β (AF-201-NA, R&D; 1:500) or anti-mouse IL-1β (500-P51, Peprotech; 1:500). Binding was detected with: anti-rabbit HRP (NA934V, GE) or anti-goat HRP (805-035-180, Jackson ImmunoResearch)(both 1:2000), ECL reagents (GE) and apposition to x-ray film (Fujifilm). Cytokines were measured using human or mouse IL-1α, IL-1β, IL-6, IL-8 and MCP-1 bead immunoassays (Life Technologies), as per the manufacturer's instructions, and assayed with a flow cytometer (Accuri C6). The antibody binding to the region between the calpain and caspase-5 cleavage site in IL-1α was generated by immunising rabbits with a KLH conjugated peptide, followed by affinity purification and biotinylation (Innovagen). This was then used as the detection reagent in a standard sandwich ELISA using a goat anti-human IL-1α antibody (R&D) as capture.

Gene expression analysis

RNA was isolated (RNeasy, Qiagen) and converted to cDNA using AMV reverse transcriptase (Promega). qPCR used Taqman probes with Amplitaq Gold (Life Technologies) in a RotorGene thermocycler (Corbett). Gene expression was evaluated using the $2^{-\Delta\Delta CT}$ method using GUSB as a reference gene. qPCR data is displayed as $2^{-\Delta\Delta CT}$, but statistical analysis was performed on the untransformed $\Delta\Delta CT$ values. RNA-Seq data was from GEO GSE72404.

Assessment of Cell Surface IL-1α

Cells were detached (Accutase), fixed (2% formaldehyde; 5 mins, RT), washed (BSA, 0.5%; NaN₃, 0.05%; in PBS), Fc blocked (10 mins, RT; Biolegend; 1:100), before incubation (30 mins, RT) with anti-IL-1α-FITC (FAB200F, R&D; 1:20) or isotype control-FITC (IC002F, R&D; 1:20), before washing and analysis by flow cytometry (Accuri C6).

SAβG, BrdU and SAHF staining

For SAβG staining cells were washed (PBS), fixed (0.5% glutaraldehyde, 10 mins, RT), washed (MgCl₂ 1mM/PBS) and stained in X-gal solution (X-gal, 1mg/ml; K₃Fe[CN]₆, 0.12mM; K₄Fe[CN]₆, 0.12mM; MgCl₂, 1mM; in PBS, pH 6.0) overnight (37°C). For BrdU and SAHF cells were incubated (6 h, 37°C) with 5-Bromo-2'-deoxyuridine (BrdU; 100µg/ml), fixed (4% formaldehyde; 15 mins, RT), permeabilised (0.2% Triton X-100/PBS), blocked (0.5% goat serum), and incubation with anti-BrdU (555627, BD; 1:500), washed (Tween 0.05%/PBS; 5 mins) and incubated (1 h) with goat anti-mouse Alexa-488 (A-11034, Thermo Fisher; 1:500). Cells were mounted in VECTASHIELD (Vector Laboratories) with DAPI (1µg/ml) and imaged with a TCS SP8 microscope (Leica).

Immunofluorescence and Immunohistochemistry

After processing paraffin sections were cleared before antigen retrieval with sodium citrate (10mM; pH 6), blocking with M.O.M. (Vector Laboratories) and donkey serum (0.5%, 1 h), and then incubated (4°C, 16 h) with antibodies to: anti-NRAS (sc-31, Santa Cruz; 1:250), anti-caspase-11 (MAB86481, R&D; 1:50), anti-F4/80 (MCA497, Serotec; 1:100) and anti-Ki67 (GTX16667, GeneTex; 1:500). After washing (Tween 0.05%/PBS; 5 mins) primary antibodies were visualised with donkey anti-rat Alexa-488 (ab150153, Abcam), donkey anti-mouse Alexa-647 (A31571, Invitrogen), donkey anti-rabbit Alexa-555 (A31572, Invitrogen; all 1:250) or the EnVision+ kit (K500711-2, Agilent Technologies).

Autofluorescence was reduced by incubation (10 mins, RT) with Sudan Black (0.1% in 70% EtOH) before mounting in VECTASHIELD (Vector Laboratories) with DAPI (1 μ g/ml), or counterstained with haematoxylin. Slides were imaged or scanned on an Aperio AT2 (Leica). Images were analysed with HALO (Indica Labs) and the Cytonuclear v1.4 algorithm.

Statistical Analysis

All statistical analyses were carried out using Prism 7 (Graphpad). Data was analysed by unpaired t-test (two-tailed), one-way ANOVA with Dunnett's post hoc or one-way ANOVA with Tukey's post-hoc. n = individual biological replicate performed in duplicate. The *in vitro* experiments typically required sample sizes of n = 3-4 to provide adequate power, and produced data that was normally distributed.

Data availability

The data that support the findings of this study are available from the corresponding author upon reasonable request.

REFERENCES

- Acosta, J. C., Banito, A., Wuestefeld, T., Georgilis, A., Janich, P., Morton, J. P., . . . Gil, J. (2013). A complex secretory program orchestrated by the inflammasome controls paracrine senescence. *Nat Cell Biol*, 15(8), 978-990.
- Afonina, I. S., Tynan, G. A., Logue, S. E., Cullen, S. P., Bots, M., Luthi, A. U., . . . Martin, S. J. (2011). Granzyme B-dependent proteolysis acts as a switch to enhance the proinflammatory activity of IL-1alpha. *Mol Cell*, 44(2), 265-278.
- Baker, D. J., Childs, B. G., Durik, M., Wijers, M. E., Sieben, C. J., Zhong, J., . . . van Deursen, J. M. (2016). Naturally occurring p16(Ink4a)-positive cells shorten healthy lifespan. *Nature*, 530(7589), 184-189. doi:10.1038/nature16932
- Baker, D. J., Wijshake, T., Tchkonina, T., LeBrasseur, N. K., Childs, B. G., van de Sluis, B., . . . van Deursen, J. M. (2011). Clearance of p16Ink4a-positive senescent cells delays ageing-associated disorders. *Nature*, 479(7372), 232-236. doi:10.1038/nature10600
- Black, R. A., Kronheim, S. R., Cantrell, M., Deeley, M. C., March, C. J., Prickett, K. S., . . . et al. (1988). Generation of biologically active interleukin-1 beta by proteolytic cleavage of the inactive precursor. *J Biol Chem*, 263(19), 9437-9442.
- Burzynski, L. C., Humphry, M., Bennett, M. R., & Clarke, M. C. (2015). Interleukin-1alpha Activity in Necrotic Endothelial Cells Is Controlled by Caspase-1 Cleavage of Interleukin-1 Receptor-2: IMPLICATIONS FOR ALLOGRAFT REJECTION. *J Biol Chem*, 290(41), 25188-25196. doi:10.1074/jbc.M115.667915
- Childs, B. G., Baker, D. J., Wijshake, T., Conover, C. A., Campisi, J., & van Deursen, J. M. (2016). Senescent intimal foam cells are deleterious at all stages of atherosclerosis. *Science*, 354(6311), 472-477. doi:10.1126/science.aaf6659
- Coppe, J. P., Patil, C. K., Rodier, F., Sun, Y., Munoz, D. P., Goldstein, J., . . . Campisi, J. (2008). Senescence-associated secretory phenotypes reveal cell-nonautonomous functions of oncogenic RAS and the p53 tumor suppressor. *PLoS Biol*, 6(12), 2853-2868.
- Dauch, D., Rudalska, R., Cossa, G., Nault, J. C., Kang, T. W., Wuestefeld, T., . . . Zender, L. (2016). A MYC-aurora kinase A protein complex represents an actionable drug target in p53-altered liver cancer. *Nat Med*, 22(7), 744-753. doi:10.1038/nm.4107
- Dinarello, C. A. (2009). Immunological and inflammatory functions of the interleukin-1 family. *Annu Rev Immunol*, 27, 519-550.
- Gardner, S. E., Humphry, M., Bennett, M. R., & Clarke, M. C. (2015). Senescent Vascular Smooth Muscle Cells Drive Inflammation Through an Interleukin-1alpha-Dependent Senescence-Associated Secretory Phenotype. *Arterioscler Thromb Vasc Biol*, 35(9), 1963-1974. doi:10.1161/ATVBAHA.115.305896
- Gluck, S., Guey, B., Gulen, M. F., Wolter, K., Kang, T. W., Schmacke, N. A., . . . Ablasser, A. (2017). Innate immune sensing of cytosolic chromatin fragments through cGAS promotes senescence. *Nat Cell Biol*, 19(9), 1061-1070. doi:10.1038/ncb3586
- Grivennikov, S. I., Greten, F. R., & Karin, M. (2010). Immunity, inflammation, and cancer. *Cell*, 140(6), 883-899. doi:10.1016/j.cell.2010.01.025
- Jeon, O. H., Kim, C., Laberge, R. M., Demaria, M., Rathod, S., Vasserot, A. P., . . . Elisseff, J. H. (2017). Local clearance of senescent cells attenuates the development of post-traumatic osteoarthritis and creates a pro-regenerative environment. *Nat Med*, 23(6), 775-781. doi:10.1038/nm.4324
- Jung, Y., Wen, T., Mingler, M. K., Caldwell, J. M., Wang, Y. H., Chaplin, D. D., . . . Rothenberg, M. E. (2015). IL-1beta in eosinophil-mediated small intestinal homeostasis and IgA production. *Mucosal Immunol*, 8(4), 930-942. doi:10.1038/mi.2014.123
- Kajiwara, Y., Schiff, T., Voloudakis, G., Gama Sosa, M. A., Elder, G., Bozdagi, O., & Buxbaum, J. D. (2014). A critical role for human caspase-4 in endotoxin sensitivity. *J Immunol*, 193(1), 335-343. doi:10.4049/jimmunol.1303424
- Kang, C., Xu, Q., Martin, T. D., Li, M. Z., Demaria, M., Aron, L., . . . Elledge, S. J. (2015). The DNA damage response induces inflammation and senescence by inhibiting autophagy of GATA4. *Science*, 349(6255), aaa5612. doi:10.1126/science.aaa5612

- Kang, T. W., Yevsa, T., Woller, N., Hoenicke, L., Wuestefeld, T., Dauch, D., . . . Zender, L. (2011). Senescence surveillance of pre-malignant hepatocytes limits liver cancer development. *Nature*, 479(7374), 547-551. doi:10.1038/nature10599
- Kayagaki, N., Stowe, I. B., Lee, B. L., O'Rourke, K., Anderson, K., Warming, S., . . . Dixit, V. M. (2015). Caspase-11 cleaves gasdermin D for non-canonical inflammasome signalling. *Nature*, 526(7575), 666-671. doi:10.1038/nature15541
- Kayagaki, N., Warming, S., Lamkanfi, M., Vande Walle, L., Louie, S., Dong, J., . . . Dixit, V. M. (2011). Non-canonical inflammasome activation targets caspase-11. *Nature*, 479(7371), 117-121. doi:10.1038/nature10558
- Kayagaki, N., Wong, M. T., Stowe, I. B., Ramani, S. R., Gonzalez, L. C., Akashi-Takamura, S., . . . Dixit, V. M. (2013). Noncanonical inflammasome activation by intracellular LPS independent of TLR4. *Science*, 341(6151), 1246-1249. doi:10.1126/science.1240248
- Kim, B., Lee, Y., Kim, E., Kwak, A., Ryoo, S., Bae, S. H., . . . Dinarello, C. A. (2013). The Interleukin-1alpha Precursor is Biologically Active and is Likely a Key Alarmin in the IL-1 Family of Cytokines. *Front Immunol*, 4, 391.
- Kuida, K., Lippke, J., Ku, G., Harding, M., Livingston, D., Su, M., & Flavell, R. (1995). Altered cytokine export and apoptosis in mice deficient in interleukin-1-beta converting enzyme. *Science*, 267, 2000-2003.
- Laberge, R. M., Sun, Y., Orjalo, A. V., Patil, C. K., Freund, A., Zhou, L., . . . Campisi, J. (2015). MTOR regulates the pro-tumorigenic senescence-associated secretory phenotype by promoting IL1A translation. *Nat Cell Biol*, 17(8), 1049-1061. doi:10.1038/ncb3195
- Li, P., Allen, H., Banerjee, S., Franklin, S., Herzog, L., Johnston, C., . . . Salfeld, J. (1995). Mice deficient in IL-1 beta-converting enzyme are defective in production of mature IL-1 beta and resistant to endotoxic shock. *Cell*, 30, 401-411.
- Martinon, F., Burns, K., & Tschopp, J. (2002). The inflammasome: a molecular platform triggering activation of inflammatory caspases and processing of proIL-beta. *Mol Cell*, 10(2), 417-426.
- McCarthy, D. A., Clark, R. R., Bartling, T. R., Trebak, M., & Melendez, J. A. (2013). Redox control of the senescence regulator interleukin-1alpha and the secretory phenotype. *J Biol Chem*, 288(45), 32149-32159. doi:10.1074/jbc.M113.493841
- Munoz-Espin, D., & Serrano, M. (2014). Cellular senescence: from physiology to pathology. *Nat Rev Mol Cell Biol*, 15(7), 482-496. doi:10.1038/nrm3823
- Offman, J., Gascoigne, K., Bristow, F., Macpherson, P., Bignami, M., Casorelli, I., . . . Karran, P. (2005). Repeated sequences in CASPASE-5 and FANCD2 but not NF1 are targets for mutation in microsatellite-unstable acute leukemia/myelodysplastic syndrome. *Mol Cancer Res*, 3(5), 251-260. doi:10.1158/1541-7786.MCR-04-0182
- Orjalo, A. V., Bhaumik, D., Gengler, B. K., Scott, G. K., & Campisi, J. (2009). Cell surface-bound IL-1alpha is an upstream regulator of the senescence-associated IL-6/IL-8 cytokine network. *Proc Natl Acad Sci U S A*, 106(40), 17031-17036.
- Rosser, E. C., Oleinika, K., Tonon, S., Doyle, R., Bosma, A., Carter, N. A., . . . Mauri, C. (2014). Regulatory B cells are induced by gut microbiota-driven interleukin-1beta and interleukin-6 production. *Nat Med*, 20(11), 1334-1339. doi:10.1038/nm.3680
- Shi, J., Zhao, Y., Wang, K., Shi, X., Wang, Y., Huang, H., . . . Shao, F. (2015). Cleavage of GSDMD by inflammatory caspases determines pyroptotic cell death. *Nature*, 526(7575), 660-665. doi:10.1038/nature15514
- Shi, J., Zhao, Y., Wang, Y., Gao, W., Ding, J., Li, P., . . . Shao, F. (2014). Inflammatory caspases are innate immune receptors for intracellular LPS. *Nature*, 514(7521), 187-192. doi:10.1038/nature13683
- Sims, J. E., & Smith, D. E. (2010). The IL-1 family: regulators of immunity. *Nat Rev Immunol*, 10(2), 89-102.
- Soung, Y. H., Jeong, E. G., Ahn, C. H., Kim, S. S., Song, S. Y., Yoo, N. J., & Lee, S. H. (2008). Mutational analysis of caspase 1, 4, and 5 genes in common human cancers. *Hum Pathol*, 39(6), 895-900. doi:10.1016/j.humpath.2007.10.015

- Vigano, E., Diamond, C. E., Spreafico, R., Balachander, A., Sobota, R. M., & Mortellaro, A. (2015). Human caspase-4 and caspase-5 regulate the one-step non-canonical inflammasome activation in monocytes. *Nat Commun*, *6*, 8761. doi:10.1038/ncomms9761
- Wang, S., Miura, M., Jung, Y. K., Zhu, H., Li, E., & Yuan, J. (1998). Murine caspase-11, an ICE-interacting protease, is essential for the activation of ICE. *Cell*, *92*(4), 501-509.
- Yang, H., Wang, H., Ren, J., Chen, Q., & Chen, Z. J. (2017). cGAS is essential for cellular senescence. *Proc Natl Acad Sci U S A*, *114*(23), E4612-E4620. doi:10.1073/pnas.1705499114
- Young, A. R., Narita, M., Ferreira, M., Kirschner, K., Sadaie, M., Darot, J. F., . . . Narita, M. (2009). Autophagy mediates the mitotic senescence transition. *Genes Dev*, *23*(7), 798-803. doi:10.1101/gad.519709
- Zheng, Y., Humphry, M., Maguire, J. J., Bennett, M. R., & Clarke, M. C. (2013). Intracellular interleukin-1 receptor 2 binding prevents cleavage and activity of interleukin-1alpha, controlling necrosis-induced sterile inflammation. *Immunity*, *38*(2), 285-295.

ACKNOWLEDGEMENTS

Work was funded by British Heart Foundation grants FS/13/3/30038, FS/18/19/33371 and RG/16/8/32388 (MC); Cancer Research UK Cambridge Institute Core Grant C14303/A17197, Medical Research Council grants MR/M013049/1 and MR/R010013/1 (MN); and the Cambridge NIHR Biomedical Research Centre. We thank the Chilver's group for monocytes, Tae-Won Kang, Lars Zender and Matthew Hoare for reagents and technical support.

AUTHOR CONTRIBUTIONS

KW, AP, LC, SW and MH designed and performed experiments, and analysed data. JG and MN designed experiments, analysed data and provided helpful discussions. MC conceived the project, designed experiments, analysed data, and wrote the manuscript with KW.

COMPETING INTERESTS

All authors declare no conflicting interests, financial or otherwise.

FIGURE LEGENDS

Figure 1: Caspase-5 cleavage of human IL-1 α at a conserved site increases activity. (a) Western blot for IL-1 α after incubation of pro-IL-1 α with active caspases, or alone (incubation control; IC). (b) IL-1-dependent IL-6 production by HeLa cells treated with reaction products from pro-IL-1 α incubated \pm active caspases, \pm neutralising IL-1 α antibody (α pAb). (c,d) Western blot (c) and bioactivity (d) of IL-1 α after incubation \pm caspase-5, \pm caspase inhibitor LEVD. (e) Multi species IL-1 α protein alignment showing conserved aspartic acid residue (arrow). (f) Western blot for wild-type (WT) or mutant D¹⁰³A pro-IL-1 α after incubation \pm caspase-5, or alone (IC). (g) IL-1-dependent IL-6 production by HeLa cells treated with reaction products from WT or mutant pro-IL-1 α incubated \pm caspase-5, \pm neutralising IL-1 α antibody (α pAb). (h) Pictograph showing position of cleavage sites in IL-1 α . Data represent mean \pm s.e.m. of n = 3 (g), n = 4 (b,d); p = ** \leq 0.01, *** \leq 0.001, **** \leq 0.0001; ns = not significant.

Figure 2: Release of cleaved IL-1 α from human cells requires caspase-5. (a-d) ELISA data showing detection of recombinant pro (p33), calpain cleaved (p17), or non-calpain cleaved (>p17) IL-1 α (a), the level of total cleaved IL-1 α (b) or non-calpain cleaved IL-1 α (c) in the conditioned media of HeLa cells transfected with WT or D¹⁰³A pro-IL-1 α and treated with intracellular LPS (icLPS), or total cleavage of WT or D¹⁰³A pro-IL-1 α by calpain (d). (e) Western blot for IL-1 α in HeLa cells transfected with WT or D¹⁰³A pro-IL-1 α , \pm icLPS treatment. (f,g) ELISA data showing level of non-calpain cleaved IL-1 α in the conditioned media of LPS primed human monocyte-derived macrophages (hMDMs) after icLPS (f) or ATP (g) treatment. (h) qPCR data showing relative gene expression in hMDMs after transfection of control or *CASP5*-targeted siRNA. (i,j) ELISA data showing level of total cleaved IL-1 α (i) or non-calpain cleaved IL-1 α (j) in the conditioned media of icLPS treated hMDMs after transfection of control or *CASP5*-targeted siRNA. Data represent mean \pm s.e.m. of n = 3 (b-d), n = 4 (h-j), or mean \pm s.d. of n = 3 separate donors (f,g); p = * \leq 0.05, ** \leq 0.01, *** \leq 0.001; ns = not significant, nd = not detected.

Figure 3: Release of cleaved IL-1 α from murine macrophages requires caspase-11. (a,b) qPCR data showing changes in *CASP4*, *CASP5* (a) or *Casp11* (b) transcript after LPS treatment of primary human (a) or mouse (b) macrophages. (c) Western blot for IL-1 α after incubation of murine pro-IL-1 α with murine caspase-1, or alone (IC). (d) IL-1-dependent IL-6 production by murine fibroblasts treated with reaction products from murine pro-IL-1 α incubated \pm murine caspase-1. (e,f) Western blot of murine wild-type (WT) or D¹⁰⁶A pro-IL-1 α (e) and bioactivity of murine WT pro-IL-1 α (f) after incubation \pm caspase-11. (g-l) ELISA data showing the level of cleaved IL-1 α (g,i,k) or IL-1 β (h,j,l) detected in the conditioned media of mouse bone marrow-derived macrophages (mBMDMs) from WT, *Casp11*^{-/-} (g,h) or *Casp1*^{-/-}/*Casp11*^{Tg} (i,j) mice, or immortalised mBMDMs transfected with empty, WT *Il1a* or D106A *Il1a* vectors (k,l), followed by LPS priming and then transfection of intracellular LPS (icLPS). Data represent mean \pm s.e.m. of n = 3 (a,b,f-l), n = 4 (d); p = ** \leq 0.01, *** \leq 0.001, **** \leq 0.0001; ns = not significant.

Figure 4: Caspase-5 is required for the IL-1 α -dependent SASP. (a-c) Representative images and quantification of senescence-associated beta galactosidase (SA β G) (a), proliferation by BrdU (b), and senescence-associated heterochromatic foci (SAHF) (c) in growing (Grow.) and senescent (Sen.) IMR-90 cells (n.b. b,c are the same field of view). (d-g) Caspase-5 expression by RNA-Seq (d), cell surface IL-1 α by flow cytometry (e), cleaved IL-1 α in the conditioned media by ELISA (f), and level of cell death (g) in growing and senescent IMR-90 cells. (h) ELISA data showing the level of IL-6, \pm neutralising IL-1 α antibody (α pAb) or IL-1RA (RA) in the conditioned media of growing and senescent IMR-90 cells. (i) qPCR data showing relative expression of *CASP5* in senescent IMR-90 cells after transfection of control (Ctrl) or *CASP5*-targeted siRNAs. (j-o) Cell surface IL-1 α by flow cytometry (j), or total cleaved IL-1 α (k), non-calpain cleaved IL-1 α (l), IL-6 (m), IL-8 (n) and MCP-1 (o) by ELISA in the conditioned media of senescent IMR-90 cells after transfection of control or *CASP5*-targeted siRNA. Data represent mean \pm s.e.m. of n = 3, n = 4 (n,o), n = 6 (d); p = * \leq 0.05, ** \leq 0.01, *** \leq 0.001, **** \leq 0.0001; ns = not significant. Scale bars = 100 μ m (a), 15 μ m (b,c).

Figure 5: Caspase-11 is required for immune surveillance of senescent cells *in vivo*. (a-d) Representative images (a,c) and quantification (b,d) of caspase-11 (green) and NRAS (magenta) staining in individual liver cells 6 days after hydrodynamic tail vein injection of NRAS with control (a,b) or *Casp11*-targeted (c,d) shRNA constructs. White arrows indicate NRAS +ve/caspase-11 -ve cells (c). (e) qPCR data showing the level of *Casp11* expression in livers 3 days after injection of constructs as indicated. (f,g) Representative images (f) and quantification (g) of NRAS staining (brown) in livers after the time and injection of constructs as indicated. (h) Quantification of F4/80 staining in livers treated as indicated. (i) Quantification of number of Ki67/NRAS double +ve cells in livers 6 days after injection of constructs. Data represent mean \pm s.e.m. of n = 5 (b,d,e,h,i), or as indicated (g); p = * \leq 0.05, ** \leq 0.01, **** \leq 0.0001; ns = not significant. Scale bars = 50 μ m (a,c), 300 μ m (f).

SUPPLEMENTAL FIGURE LEGENDS (Not included in word count)

Supplementary Figure 1: (a) Schematic showing location of the custom peptide antibody relative to the calpain and caspase-5 cleavage sites in pro-IL-1 α . (b-c) Data showing specificity of our custom non-calpain cleaved IL-1 α ELISA (b) or a total cleaved IL-1 α ELISA (c) for detecting either calpain or caspase-5 cleaved pro-IL-1 α . IC = incubation control (no enzyme); +E = +enzyme. Data represent mean \pm s.e.m. of n = 3; p = *** \leq 0.001, **** \leq 0.0001.

Supplementary Figure 2: (a) Western blot for IL-1 β after incubation of murine pro-IL-1 β with murine caspase-1, or alone (IC). (b) IL-1-dependent IL-6 production by murine fibroblasts treated with reaction products from murine pro-IL-1 β incubated \pm murine caspase-1. Data represent mean \pm s.e.m. of n = 4; p = **** \leq 0.0001.

Supplementary Figure 3: (a,b) Analysis of cell viability by release of lactate dehydrogenase (LDH) into the conditioned media (a) and number of cells attached by crystal violet staining (b) in immortalised mBMDMs after transfection of empty, WT *Il1a* or D106A *Il1a* vectors, followed by LPS priming and then transfection of intracellular LPS (icLPS). Data represent mean \pm s.d. of n = 3; ns = not significant.

Supplementary Figure 4: Representative flow cytometry dot plots of growing IMR-90 cells, senescent IMR-90 cells and senescent IMR-90 cells after CASP5 knockdown, which were left unstained or stained with isotype control-FITC or anti-IL-1 α -FITC antibodies before analysis by flow cytometry.

Supplementary Figure 5: ELISA data showing the level of IL-8 and MCP-1 in the conditioned media of growing (Grow.) or senescent (Sen.) IMR-90 cells, \pm neutralising IL-1 α antibody (α pAb). Data represent mean \pm s.e.m. of n = \geq 3; p = **** \leq 0.0001.

Supplementary Figure 6: (a) Western blot for IL-1 β in growing (Grow.) and senescent (Sen.) IMR-90 cells. (b) ELISA data showing the level of IL-1 β in the conditioned media of growing and senescent IMR-90 cells. Grey dotted line indicates limit of detection. Data represent mean \pm s.e.m. of n = 3.

Supplementary Figure 7: (a) Representative images and quantification of senescence-associated beta galactosidase (SA β G) staining in growing (Grow.) and senescent (Sen.) WI-38 cells. (b,c) ELISA data showing the level of cleaved IL-1 α and/or SASP factors in the conditioned media of growing and senescent WI-38 cells (b), or senescent WI-38 cells \pm neutralising IL-1 α antibody (α pAb) (c). (d,e) Relative *CASP5* expression by qPCR (d) or SASP factors in the conditioned media by ELISA (e) in senescent WI-38 cells after transfection of control (Ctrl) or *CASP5*-targeted siRNA. Data represent mean \pm s.e.m. of n = \geq 3 (a,c-e); or mean \pm s.d. of n=2 (b); p = * \leq 0.05, ** \leq 0.01, *** \leq 0.001, **** \leq 0.0001.

Supplementary Figure 8: (a,b) Level of SA β G and BrdU +ve cells in senescent IMR-90 (a) and WI-38 (b) cell cultures after transfection of control (Ctrl) or *CASP5*-targeted siRNAs. Data represent mean \pm s.d. representative of n = 2.

Supplementary Figure 9: (a) qPCR data showing relative expression of cGAS in senescent IMR-90 cells after transfection of control or *cGAS*-targeted siRNAs. (b-d) Total cleaved IL-1 α (b) and IL-6 (c) by ELISA in the conditioned media, or *CASP5* expression by qPCR (d) in senescent IMR-90 cells after transfection of control or *cGAS*-targeted siRNAs. Data represent mean \pm s.e.m. of n = 3 (a-c), n = 6 (d); p = * \leq 0.05, **** \leq 0.0001.

Supplementary Figure 10: Linear regression analysis of the correlation between average caspase-11 staining intensity and percentage of RAS positive cells in mouse livers 6 days after injection.

Supplementary Figure 11: (a) Representative images of immune cells clustering around two NRAS+ senescent cells (arrows) within mouse liver 6 days after hydrodynamic tail vein injection of NRAS. (b) Quantification of immune cell clusters around NRAS+ cells within mouse liver 6 days after hydrodynamic tail vein injection of NRAS with control (Ctrl) or *Casp11*-targeted shRNA constructs. Data represent mean \pm s.d. of n = 5 mice; p = ** \leq 0.01.